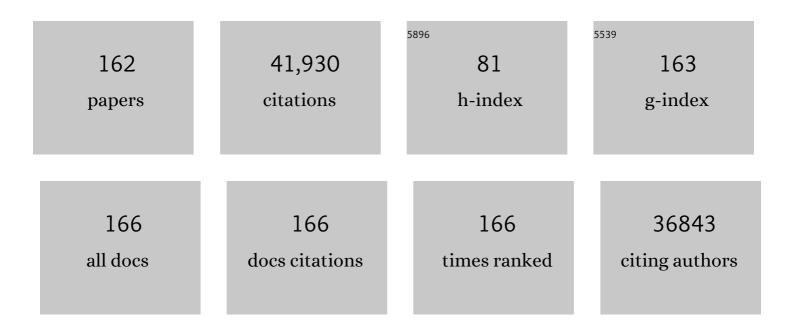


List of Publications by Year in descending order

Source: https://exaly.com/author-pdf/4713987/publications.pdf Version: 2024-02-01



#	Article	IF	CITATIONS
1	Large-Area Synthesis of High-Quality and Uniform Graphene Films on Copper Foils. Science, 2009, 324, 1312-1314.	12.6	10,000
2	Chemically Derived, Ultrasmooth Graphene Nanoribbon Semiconductors. Science, 2008, 319, 1229-1232.	12.6	4,504
3	A review on g-C 3 N 4 -based photocatalysts. Applied Surface Science, 2017, 391, 72-123.	6.1	2,318
4	N-Doping of Graphene Through Electrothermal Reactions with Ammonia. Science, 2009, 324, 768-771.	12.6	2,020
5	Engineering heterogeneous semiconductors for solar water splitting. Journal of Materials Chemistry A, 2015, 3, 2485-2534.	10.3	1,609
6	Cocatalysts for Selective Photoreduction of CO ₂ into Solar Fuels. Chemical Reviews, 2019, 119, 3962-4179.	47.7	1,591
7	Hierarchical photocatalysts. Chemical Society Reviews, 2016, 45, 2603-2636.	38.1	1,517
8	Graphene in Photocatalysis: A Review. Small, 2016, 12, 6640-6696.	10.0	836
9	CdS/Graphene Nanocomposite Photocatalysts. Advanced Energy Materials, 2015, 5, 1500010.	19.5	694
10	Photocatalysis fundamentals and surface modification of TiO2 nanomaterials. Chinese Journal of Catalysis, 2015, 36, 2049-2070.	14.0	458
11	Design and fabrication of semiconductor photocatalyst for photocatalytic reduction of CO2 to solar fuel. Science China Materials, 2014, 57, 70-100.	6.3	446
12	Graphene-based heterojunction photocatalysts. Applied Surface Science, 2018, 430, 53-107.	6.1	386
13	A review on heterogeneous photocatalysis for environmental remediation: From semiconductors to modification strategies. Chinese Journal of Catalysis, 2022, 43, 178-214.	14.0	382
14	A review on 2D MoS2 cocatalysts in photocatalytic H2 production. Journal of Materials Science and Technology, 2020, 56, 89-121.	10.7	364
15	A Graphene-like Oxygenated Carbon Nitride Material for Improved Cycle-Life Lithium/Sulfur Batteries. Nano Letters, 2015, 15, 5137-5142.	9.1	358
16	Highly enhanced photocatalytic degradation of methylene blue over the indirect all-solid-state Z-scheme g-C3N4-RGO-TiO2 nanoheterojunctions. Applied Surface Science, 2017, 405, 60-70.	6.1	328
17	Constructing Multifunctional Metallic Ni Interface Layers in the g-C ₃ N ₄ Nanosheets/Amorphous NiS Heterojunctions for Efficient Photocatalytic H ₂ Generation. ACS Applied Materials & Interfaces, 2017, 9, 14031-14042.	8.0	319
18	Enhanced photocatalytic H ₂ evolution over noble-metal-free NiS cocatalyst modified CdS nanorods/g-C ₃ N ₄ heterojunctions. Journal of Materials Chemistry A, 2015, 3, 18244-18255.	10.3	306

#	Article	IF	CITATIONS
19	Adsorption of CO2 on heterostructure CdS(Bi2S3)/TiO2 nanotube photocatalysts and their photocatalytic activities in the reduction of CO2 to methanol under visible light irradiation. Chemical Engineering Journal, 2012, 180, 151-158.	12.7	302
20	Constructing 2D layered hybrid CdS nanosheets/MoS 2 heterojunctions for enhanced visible-light photocatalytic H 2 generation. Applied Surface Science, 2017, 391, 580-591.	6.1	284
21	Nanostructured CdS for efficient photocatalytic H2 evolution: A review. Science China Materials, 2020, 63, 2153-2188.	6.3	281
22	Constructing low-cost Ni3C/twin-crystal Zn0.5Cd0.5S heterojunction/homojunction nanohybrids for efficient photocatalytic H2 evolution. Chinese Journal of Catalysis, 2021, 42, 25-36.	14.0	272
23	A new heterojunction in photocatalysis: S-scheme heterojunction. Chinese Journal of Catalysis, 2021, 42, 667-669.	14.0	260
24	In-situ construction of metallic Ni3C@Ni core–shell cocatalysts over g-C3N4 nanosheets for shell-thickness-dependent photocatalytic H2 production. Applied Catalysis B: Environmental, 2021, 291, 120104.	20.2	258
25	Noble-metal-free Ni3C cocatalysts decorated CdS nanosheets for high-efficiency visible-light-driven photocatalytic H2 evolution. Applied Catalysis B: Environmental, 2018, 227, 218-228.	20.2	248
26	Integration of 2D layered CdS/WO3 S-scheme heterojunctions and metallic Ti3C2 MXene-based Ohmic junctions for effective photocatalytic H2 generation. Chinese Journal of Catalysis, 2022, 43, 359-369.	14.0	246
27	Bifunctional Cu ₃ P Decorated g-C ₃ N ₄ Nanosheets as a Highly Active and Robust Visible-Light Photocatalyst for H ₂ Production. ACS Sustainable Chemistry and Engineering, 2018, 6, 4026-4036.	6.7	243
28	Multi-functional Ni ₃ C cocatalyst/g-C ₃ N ₄ nanoheterojunctions for robust photocatalytic H ₂ evolution under visible light. Journal of Materials Chemistry A, 2018, 6, 13110-13122.	10.3	241
29	Ni-based photocatalytic H2-production cocatalysts2. Chinese Journal of Catalysis, 2019, 40, 240-288.	14.0	239
30	Enhanced visible light photocatalytic H2 production over Z-scheme g-C3N4 nansheets/WO3 nanorods nanocomposites loaded with Ni(OH) cocatalysts. Chinese Journal of Catalysis, 2017, 38, 240-252.	14.0	237
31	Rationally designed Ta3N5/BiOCl S-scheme heterojunction with oxygen vacancies for elimination of tetracycline antibiotic and Cr(VI): Performance, toxicity evaluation and mechanism insight. Journal of Materials Science and Technology, 2022, 123, 177-190.	10.7	232
32	<i>In situ</i> construction of a C ₃ N ₅ nanosheet/Bi ₂ WO ₆ nanodot S-scheme heterojunction with enhanced structural defects for the efficient photocatalytic removal of tetracycline and Cr(<scp>vi</scp>). Inorganic Chemistry Frontiers, 2022, 9, 2479-2497.	6.0	217
33	Fabricating the Robust g-C ₃ N ₄ Nanosheets/Carbons/NiS Multiple Heterojunctions for Enhanced Photocatalytic H ₂ Generation: An Insight into the Trifunctional Roles of Nanocarbons. ACS Sustainable Chemistry and Engineering, 2017, 5, 2224-2236.	6.7	214
34	Design and application of active sites in g-C3N4-based photocatalysts. Journal of Materials Science and Technology, 2020, 56, 69-88.	10.7	211
35	Amorphous Co ₃ O ₄ modified CdS nanorods with enhanced visible-light photocatalytic H ₂ -production activity. Dalton Transactions, 2015, 44, 1680-1689.	3.3	204
36	In situ one-pot fabrication of g-C 3 N 4 nanosheets/NiS cocatalyst heterojunction with intimate interfaces for efficient visible light photocatalytic H 2 generation. Applied Surface Science, 2018, 430, 208-217.	6.1	204

#	Article	IF	CITATIONS
37	Enhanced visible-light H2 evolution of g-C3N4 photocatalysts via the synergetic effect of amorphous NiS and cheap metal-free carbon black nanoparticles as co-catalysts. Applied Surface Science, 2015, 358, 204-212.	6.1	203
38	Facile fabrication of TaON/Bi2MoO6 core–shell S-scheme heterojunction nanofibers for boosting visible-light catalytic levofloxacin degradation and Cr(VI) reduction. Chemical Engineering Journal, 2022, 428, 131158.	12.7	203
39	Enhanced Solar Fuel H ₂ Generation over g-C ₃ N ₄ Nanosheet Photocatalysts by the Synergetic Effect of Noble Metal-Free Co ₂ P Cocatalyst and the Environmental Phosphorylation Strategy. ACS Sustainable Chemistry and Engineering, 2018, 6, 816-826.	6.7	201
40	Integrating 2D/2D CdS/α-Fe2O3 ultrathin bilayer Z-scheme heterojunction with metallic β-NiS nanosheet-based ohmic-junction for efficient photocatalytic H2 evolution. Applied Catalysis B: Environmental, 2020, 266, 118619.	20.2	199
41	Two-Dimensional Transition Metal MXene-Based Photocatalysts for Solar Fuel Generation. Journal of Physical Chemistry Letters, 2019, 10, 3488-3494.	4.6	193
42	Engineering MPx (M = Fe, Co or Ni) interface electron transfer channels for boosting photocatalytic H2 evolution over g-C3N4/MoS2 layered heterojunctions. Applied Catalysis B: Environmental, 2019, 252, 250-259.	20.2	188
43	Highly efficient visible-light photocatalytic H2 evolution over 2D–2D CdS/Cu7S4 layered heterojunctions. Chinese Journal of Catalysis, 2020, 41, 31-40.	14.0	177
44	In Situ Fabrication of Robust Cocatalystâ€Free CdS/g ₃ N ₄ 2D–2D Stepâ€6cheme Heterojunctions for Highly Active H ₂ Evolution. Solar Rrl, 2020, 4, 1900423.	5.8	176
45	Strongly coupled 2D-2D nanojunctions between P-doped Ni2S (Ni2SP) cocatalysts and CdS nanosheets for efficient photocatalytic H2 evolution. Chemical Engineering Journal, 2020, 390, 124496.	12.7	174
46	Review on design and evaluation of environmental photocatalysts. Frontiers of Environmental Science and Engineering, 2018, 12, 1.	6.0	170
47	Surface and interface engineering of hierarchical photocatalysts. Applied Surface Science, 2019, 471, 43-87.	6.1	170
48	Encapsulation of Ni ₃ Fe Nanoparticles in Nâ€Doped Carbon Nanotube–Grafted Carbon Nanofibers as Highâ€Efficiency Hydrogen Evolution Electrocatalysts. Advanced Functional Materials, 2018, 28, 1805828.	14.9	168
49	Heterogeneous sulfur-free hydrodeoxygenation catalysts for selectively upgrading the renewable bio-oils to second generation biofuels. Renewable and Sustainable Energy Reviews, 2018, 82, 3762-3797.	16.4	164
50	Synthesis and photoactivity of nanostructured CdS–TiO2 composite catalysts. Catalysis Today, 2014, 225, 64-73.	4.4	159
51	Sulfur-doped g-C3N4/g-C3N4 isotype step-scheme heterojunction for photocatalytic H2 evolution. Journal of Materials Science and Technology, 2022, 118, 15-24.	10.7	159
52	Porous graphitic carbon nitride for solar photocatalytic applications. Nanoscale Horizons, 2020, 5, 765-786.	8.0	152
53	C ₆₀ -Decorated CdS/TiO ₂ Mesoporous Architectures with Enhanced Photostability and Photocatalytic Activity for H ₂ Evolution. ACS Applied Materials & Interfaces, 2015, 7, 4533-4540.	8.0	148
54	Photoreduction of CO2 to methanol over Bi2S3/CdS photocatalyst under visible light irradiation. Journal of Natural Gas Chemistry, 2011, 20, 413-417.	1.8	145

#	Article	IF	CITATIONS
55	Synthesis, properties, and applications of black titanium dioxide nanomaterials. Science Bulletin, 2017, 62, 431-441.	9.0	134
56	Low-Cost Ni ₃ B/Ni(OH) ₂ as an Ecofriendly Hybrid Cocatalyst for Remarkably Boosting Photocatalytic H ₂ Production over g-C ₃ N ₄ Nanosheets. ACS Sustainable Chemistry and Engineering, 2018, 6, 13140-13150.	6.7	131
57	Photocatalytic reduction of carbon dioxide to methanol by Cu2O/SiC nanocrystallite under visible light irradiation. Journal of Natural Gas Chemistry, 2011, 20, 145-150.	1.8	127
58	Graphitic carbon nitride nanosheets for microwave absorption. Materials Today Physics, 2018, 5, 78-86.	6.0	127
59	Improved visible-light photocatalytic H2 generation over CdS nanosheets decorated by NiS2 and metallic carbon black as dual earth-abundant cocatalysts. Chinese Journal of Catalysis, 2017, 38, 1970-1980.	14.0	124
60	Earth-abundant NiS co-catalyst modified metal-free mpg-C ₃ N ₄ /CNT nanocomposites for highly efficient visible-light photocatalytic H ₂ evolution. Dalton Transactions, 2015, 44, 18260-18269.	3.3	123
61	Enhanced photocatalytic H2 evolution based on a Ti3C2/Zn0.7Cd0.3S/Fe2O3 Ohmic/S-scheme hybrid heterojunction with cascade 2D coupling interfaces. Chemical Engineering Journal, 2022, 429, 132587.	12.7	121
62	Co1.4Ni0.6P cocatalysts modified metallic carbon black/g-C3N4 nanosheet Schottky heterojunctions for active and durable photocatalytic H2 production. Applied Surface Science, 2019, 466, 393-400.	6.1	117
63	Tracking Sâ€ S cheme Charge Transfer Pathways in Mo ₂ C/CdS H ₂ â€Evolution Photocatalysts. Solar Rrl, 2021, 5, 2100177.	5.8	117
64	Enhanced photocatalytic degradation and adsorption of methylene blue via TiO2 nanocrystals supported on graphene-like bamboo charcoal. Applied Surface Science, 2015, 358, 425-435.	6.1	115
65	Earth-abundant WC nanoparticles as an active noble-metal-free co-catalyst for the highly boosted photocatalytic H ₂ production over g-C ₃ N ₄ nanosheets under visible light. Catalysis Science and Technology, 2017, 7, 1193-1202.	4.1	114
66	Reduced Graphene Oxideâ€Modified Carbon Nanotube/Polyimide Film Supported MoS ₂ Nanoparticles for Electrocatalytic Hydrogen Evolution. Advanced Functional Materials, 2015, 25, 2693-2700.	14.9	113
67	Markedly enhanced visible-light photocatalytic H ₂ generation over g-C ₃ N ₄ nanosheets decorated by robust nickel phosphide (Ni ₁₂ P ₅) cocatalysts. Dalton Transactions, 2017, 46, 1794-1802.	3.3	111
68	Improved charge transfer by size-dependent plasmonic Au on C3N4 for efficient photocatalytic oxidation of RhB and CO2 reduction. Chinese Journal of Catalysis, 2019, 40, 928-939.	14.0	104
69	Heterogeneous Photocatalytic Activation of Persulfate for the Removal of Organic Contaminants in Water: A Critical Review. ACS ES&T Engineering, 2022, 2, 527-546.	7.6	101
70	Effects of pore sizes of porous silica gels on desorption activation energy of water vapour. Applied Thermal Engineering, 2007, 27, 869-876.	6.0	99
71	Molecularly imprinted Ag/Ag3VO4/g-C3N4 Z-scheme photocatalysts for enhanced preferential removal of tetracycline. Journal of Colloid and Interface Science, 2019, 552, 271-286.	9.4	98
72	Carbon Nanotube-Supported Cu ₃ P as High-Efficiency and Low-Cost Cocatalysts for Exceptional Semiconductor-Free Photocatalytic H ₂ Evolution. ACS Sustainable Chemistry and Engineering, 2019, 7, 3243-3250.	6.7	96

#	Article	IF	CITATIONS
73	Carbon–Graphitic Carbon Nitride Hybrids for Heterogeneous Photocatalysis. Small, 2021, 17, e2005231.	10.0	96
74	Microwave absorbing property and complex permittivity and permeability of epoxy composites containing Ni-coated and Ag filled carbon nanotubes. Composites Science and Technology, 2008, 68, 2902-2908.	7.8	95
75	Efficient visible-light photocatalytic H ₂ evolution over metal-free g-C ₃ N ₄ co-modified with robust acetylene black and Ni(OH) ₂ as dual co-catalysts. RSC Advances, 2016, 6, 31497-31506.	3.6	94
76	ZnWO4-ZnIn2S4 S-scheme heterojunction for enhanced photocatalytic H2 evolution. Journal of Materials Science and Technology, 2022, 122, 231-242.	10.7	93
77	Regulating interfacial morphology and charge-carrier utilization of Ti3C2 modified all-sulfide CdS/ZnIn2S4 S-scheme heterojunctions for effective photocatalytic H2 evolution. Journal of Materials Science and Technology, 2022, 112, 85-95.	10.7	92
78	Bridging the g-C ₃ N ₄ Nanosheets and Robust CuS Cocatalysts by Metallic Acetylene Black Interface Mediators for Active and Durable Photocatalytic H ₂ Production. ACS Applied Energy Materials, 2018, 1, 2232-2241.	5.1	88
79	Catalytic oxidation of toluene over copper and manganese based catalysts: Effect of water vapor. Catalysis Communications, 2011, 14, 15-19.	3.3	87
80	Visible-light induced photocatalytic oxidative desulfurization using BiVO4/C3N4@SiO2 with air/cumene hydroperoxide under ambient conditions. Applied Catalysis B: Environmental, 2016, 192, 72-79.	20.2	87
81	State-of-the-art recent progress in MXene-based photocatalysts: a comprehensive review. Nanoscale, 2021, 13, 9463-9504.	5.6	87
82	Construction of a multi-interfacial-electron transfer scheme for efficient CO ₂ photoreduction: a case study using CdIn ₂ S ₄ micro-flower spheres modified with Au nanoparticles and reduced graphene oxide. Journal of Materials Chemistry A, 2020, 8, 18707-18714.	10.3	86
83	Synthesis of porous ZnS, ZnO and ZnS/ZnO nanosheets and their photocatalytic properties. RSC Advances, 2017, 7, 30956-30962.	3.6	85
84	Ultra-thin SiC layer covered graphene nanosheets as advanced photocatalysts for hydrogen evolution. Journal of Materials Chemistry A, 2015, 3, 10999-11005.	10.3	80
85	Bridging Effect of S–C Bond for Boosting Electron Transfer over Cubic Hollow CoS/g-C ₃ N ₄ Heterojunction toward Photocatalytic Hydrogen Production. Langmuir, 2022, 38, 3244-3256.	3.5	78
86	Facile preparation of bioactive nanoparticle/poly(ε-caprolactone) hierarchical porous scaffolds via 3D printing of high internal phase Pickering emulsions. Journal of Colloid and Interface Science, 2019, 545, 104-115.	9.4	76
87	Metal-free carbon nanotube–SiC nanowire heterostructures with enhanced photocatalytic H ₂ evolution under visible light irradiation. Catalysis Science and Technology, 2015, 5, 2798-2806.	4.1	74
88	Fabricated rGO-modified Ag2S nanoparticles/g-C3N4 nanosheets photocatalyst for enhancing photocatalytic activity. Journal of Colloid and Interface Science, 2019, 554, 468-478.	9.4	74
89	Copper(II) imidazolate frameworks as highly efficient photocatalysts for reduction of CO2 into methanol under visible light irradiation. Journal of Solid State Chemistry, 2013, 203, 154-159.	2.9	73
90	Synthesis and visible light photocatalytic behavior of WO3 (core)/Bi2WO6 (shell). Journal of Molecular Catalysis A, 2014, 385, 106-111.	4.8	73

#	Article	IF	CITATIONS
91	Design of metal-organic frameworks (MOFs)-based photocatalyst for solar fuel production and photo-degradation of pollutants. Chinese Journal of Catalysis, 2021, 42, 872-903.	14.0	73
92	Remarkable positive effect of Cd(OH)2 on CdS semiconductor for visible-light photocatalytic H2 production. Applied Catalysis B: Environmental, 2018, 229, 8-14.	20.2	72
93	Hydrothermal synthesis and characterization of novel PbWO4 microspheres with hierarchical nanostructures and enhanced photocatalytic performance in dye degradation. Chemical Engineering Journal, 2013, 219, 86-95.	12.7	68
94	Hydrothermal synthesis of FeWO4-graphene composites and their photocatalytic activities under visible light. Applied Surface Science, 2015, 351, 474-479.	6.1	68
95	One-pot hydrothermal synthesis of SrTiO3-reduced graphene oxide composites with enhanced photocatalytic activity for hydrogen production. Journal of Molecular Catalysis A, 2016, 423, 70-76.	4.8	65
96	BiVO4/TiO2 heterojunction with enhanced photocatalytic activities and photoelectochemistry performances under visible light illumination. Materials Research Bulletin, 2019, 117, 35-40.	5.2	64
97	Preparation, characterization and photocatalytic activity of the neodymium-doped TiO2 nanotubes. Applied Surface Science, 2009, 255, 8624-8628.	6.1	63
98	Enhanced enzymatic hydrolysis of sugarcane bagasse with ferric chloride pretreatment and surfactant. Bioresource Technology, 2017, 229, 96-103.	9.6	63
99	Facile Construction of Dual p–n Junctions in CdS/Cu ₂ 0/ZnO Photoanode with Enhanced Charge Carrier Separation and Transfer Ability. ACS Omega, 2017, 2, 852-863.	3.5	62
100	Assembling Ti3C2 MXene into ZnIn2S4-NiSe2 S-scheme heterojunction with multiple charge transfer channels for accelerated photocatalytic H2 generation. Chemical Engineering Journal, 2022, 447, 137488.	12.7	62
101	Enhancing enzymatic hydrolysis of sugarcane bagasse by ferric chloride catalyzed organosolv pretreatment and Tween 80. Bioresource Technology, 2018, 258, 295-301.	9.6	61
102	Fabrication of hierarchical copper sulfide/bismuth tungstate p-n heterojunction with two-dimensional (2D) interfacial coupling for enhanced visible-light photocatalytic degradation of glyphosate. Journal of Colloid and Interface Science, 2020, 560, 293-302.	9.4	59
103	Tracking charge transfer pathways in SrTiO3/CoP/Mo2C nanofibers for enhanced photocatalytic solar fuel production. Chinese Journal of Catalysis, 2022, 43, 507-518.	14.0	59
104	Rational Construction of Strongly Coupled Metal–Metal Oxide–Graphene Nanostructure with Excellent Electrocatalytic Activity and Durability. ACS Applied Materials & Interfaces, 2014, 6, 10258-10264.	8.0	57
105	Facilitating the enzymatic saccharification of pulped bamboo residues by degrading the remained xylan and lignin–carbohydrates complexes. Bioresource Technology, 2015, 192, 471-477.	9.6	54
106	Carbon-coated Cu-TiO2 nanocomposite with enhanced photostability and photocatalytic activity. Applied Surface Science, 2019, 466, 254-261.	6.1	54
107	Electrodeposition of Cu2O/g-C3N4 heterojunction film on an FTO substrate for enhancing visible light photoelectrochemical water splitting. Chinese Journal of Catalysis, 2017, 38, 365-371.	14.0	51
108	One-pot synthesis of ZnS nanowires/Cu ₇ S ₄ nanoparticles/reduced graphene oxide nanocomposites for supercapacitor and photocatalysis applications. Dalton Transactions, 2019, 48, 2442-2454.	3.3	46

#	Article	IF	CITATIONS
109	Electrochemical and optical biosensors based on multifunctional MXene nanoplatforms: Progress and prospects. Talanta, 2021, 235, 122726.	5.5	46
110	Synthesis and characterization of Ag/TiO2-B nanosquares with high photocatalytic activity under visible light irradiation. Materials Science and Engineering B: Solid-State Materials for Advanced Technology, 2013, 178, 344-348.	3.5	45
111	Constructing 1D/2D Schottky-Based Heterojunctions between Mn _{0.2} Cd _{0.8} S Nanorods and Ti ₃ C ₂ Nanosheets for Boosted Photocatalytic H<:sub&et2<:/sub>: Evolution. Wuli Huaxue Xuebao/ Acta Physico - Chimica Sinica. 2020	4.9	44
112	Synthesis BiVO4 modified by CuO supported onto bentonite for molecular oxygen photocatalytic oxidative desulfurization of fuel under visible light. Fuel, 2021, 290, 120066.	6.4	39
113	Covalent organic frameworks: Fundamentals, mechanisms, modification, and applications in photocatalysis. Chem Catalysis, 2022, 2, 2157-2228.	6.1	39
114	Topological morphology conversion towards SnO ₂ /SiC hollow sphere nanochains with efficient photocatalytic hydrogen evolution. Chemical Communications, 2014, 50, 1070-1073.	4.1	37
115	Constructed Z-Scheme g-C ₃ N ₄ /Ag ₃ VO ₄ /rGO Photocatalysts with Multi-interfacial Electron-Transfer Paths for High Photoreduction of CO ₂ . Inorganic Chemistry, 2021, 60, 1755-1766.	4.0	37
116	Intensive photocatalytic activity enhancement of Bi 5 O 7 I via coupling with band structure and content adjustable BiOBr x I 1â~ x. Science Bulletin, 2018, 63, 219-227.	9.0	36
117	Effects of ferric chloride pretreatment and surfactants on the sugar production from sugarcane bagasse. Bioresource Technology, 2018, 265, 93-101.	9.6	36
118	Dynamics and isotherms of water vapor sorption on mesoporous silica gels modified by different salts. Kinetics and Catalysis, 2010, 51, 754-761.	1.0	35
119	Synthesis of yolk/shell Fe3O4–polydopamine–graphene–Pt nanocomposite with high electrocatalytic activity for fuel cells. Journal of Power Sources, 2014, 246, 868-875.	7.8	35
120	Design and preparation of CdS/H-3D-TiO2/Pt-wire photocatalysis system with enhanced visible-light driven H2 evolution. International Journal of Hydrogen Energy, 2017, 42, 928-937.	7.1	35
121	Adsorption Equilibrium and Desorption Activation Energy of Water Vapor on Activated Carbon Modified by an Oxidation and Reduction Treatment. Journal of Chemical & Engineering Data, 2010, 55, 3164-3169.	1.9	34
122	Graphitied carbon-coated bimetallic FeCu nanoparticles as original g-C3N4 cocatalysts for improving photocatalystic activity. Applied Surface Science, 2019, 492, 571-578.	6.1	34
123	Branch-like Cd Zn1-Se/Cu2O@Cu step-scheme heterojunction for CO2 photoreduction. Materials Today Physics, 2022, 26, 100729.	6.0	31
124	Photocatalytic Hydrogen Production over CdS Nanomaterials: An Interdisciplinary Experiment for Introducing Undergraduate Students to Photocatalysis and Analytical Chemistry. Journal of Chemical Education, 2019, 96, 1224-1229.	2.3	30
125	Highly active and selective hydrodeoxygenation of oleic acid to second generation bio-diesel over SiO2-supported CoxNi1â^'xP catalysts. Fuel, 2019, 247, 26-35.	6.4	29
126	Charge transfer and orbital reconstruction of non-noble transition metal single-atoms anchored on Ti2CT -MXenes for highly selective CO2 electrochemical reduction. Chinese Journal of Catalysis, 2022, 43, 1906-1917.	14.0	29

#	Article	IF	CITATIONS
127	Intersubunit Electron Transfer (IET) in Quantum Dots/Graphene Complex: What Features Does IET Endow the Complex with?. Journal of Physical Chemistry C, 2012, 116, 15833-15838.	3.1	28
128	G-C3N4 quantum dots and Au nano particles co-modified CeO2/Fe3O4 micro-flowers photocatalyst for enhanced CO2 photoreduction. Renewable Energy, 2021, 179, 756-765.	8.9	28
129	Facile synthesis of oil-soluble Fe3O4 nanoparticles based on a phase transfer mechanism. Applied Surface Science, 2014, 307, 306-310.	6.1	27
130	Redox shuttle enhances nonthermal femtosecond two-photon self-doping of rGO–TiO _{2â^'x} photocatalysts under visible light. Journal of Materials Chemistry A, 2018, 6, 16430-16438.	10.3	27
131	Synthesized Z-scheme photocatalyst ZnO/g-C3N4 for enhanced photocatalytic reduction of CO2. New Journal of Chemistry, 2020, 44, 16390-16399.	2.8	26
132	Smartphone-based photoelectrochemical biosensing system with graphitic carbon nitride/gold nanoparticles modified electrodes for matrix metalloproteinase-2 detection. Biosensors and Bioelectronics, 2021, 193, 113572.	10.1	26
133	Effects of Textural Properties and Surface Oxygen Content of Activated Carbons on the Desorption Activation Energy of Water. Adsorption Science and Technology, 2006, 24, 363-374.	3.2	25
134	Heterostructured CoO/3D-TiO2 nanorod arrays for photoelectrochemical water splitting hydrogen production. Journal of Solid State Electrochemistry, 2017, 21, 455-461.	2.5	25
135	Principle and surface science of photocatalysis. Interface Science and Technology, 2020, 31, 1-38.	3.3	24
136	Enhancement of photocatalytic NO removal activity of g-C ₃ N ₄ by modification with illite particles. Environmental Science: Nano, 2020, 7, 1990-1998.	4.3	23
137	Photodeposition of NiS Cocatalysts on gâ€C ₃ N ₄ with Edge Grafting of 4â€(1Hâ€Imidazolâ€2â€yl) Benzoic Acid for Highly Elevated Photocatalytic H ₂ Evolution. Advanced Sustainable Systems, 2023, 7, .	5.3	23
138	Single-crystalline melem (C ₆ N ₁₀ H ₆) nanorods: a novel stable molecular crystal photocatalyst with modulated charge potentials and dynamics. Journal of Materials Chemistry A, 2019, 7, 13234-13241.	10.3	22
139	Engineering 2D multi-hetero-interface in the well-designed nanosheet composite photocatalyst with broad electron-transfer channels for highly-efficient solar-to-fuels conversion. Applied Catalysis B: Environmental, 2021, 286, 119944.	20.2	22
140	Equilibrium and Doâ^'Do Model Fitting of Water Adsorption on Four Commercial Activated Carbons with Different Surface Chemistry and Pore Structure. Journal of Chemical & Engineering Data, 2010, 55, 5729-5732.	1.9	21
141	Rational design of Z-scheme Bi12O17Cl2/plasmonic Ag/anoxic TiO2 composites for efficient visible light photocatalysis. Powder Technology, 2021, 384, 342-352.	4.2	20
142	Urea-induced supramolecular self-assembly strategy to synthesize wrinkled porous carbon nitride nanosheets for highly-efficient visible-light photocatalytic degradation. RSC Advances, 2021, 11, 23459-23470.	3.6	19
143	Novel 3-D nanoporous graphitic-C3N4 nanosheets with heterostructured modification for efficient visible-light photocatalytic hydrogen production. RSC Advances, 2014, 4, 52332-52337.	3.6	18
144	Preparation of W and N, S-codoped titanium dioxide with enhanced photocatalytic activity under visible light irradiation. Materials Research Bulletin, 2016, 76, 72-78.	5.2	18

#	Article	IF	CITATIONS
145	Facile preparation of biocompatible poly(l-lactic acid)-modified halloysite nanotubes/poly(Îμ-caprolactone) porous scaffolds by solvent evaporation of Pickering emulsion templates. Journal of Materials Science, 2018, 53, 14774-14788.	3.7	18
146	Fabricating intramolecular donor-acceptor system via covalent bonding of carbazole to carbon nitride for excellent photocatalytic performance towards CO2 conversion. Journal of Colloid and Interface Science, 2021, 594, 550-560.	9.4	18
147	Photocatalytic Reduction of CO ₂ Using TiO ₂ -Graphene Nanocomposites. Journal of Nanomaterials, 2016, 2016, 1-5.	2.7	17
148	Surface and interface modification strategies of CdS-based photocatalysts. Interface Science and Technology, 2020, , 313-348.	3.3	17
149	Fabrication of sustainedâ€release and antibacterial citronella oilâ€loaded composite microcapsules based on <scp>P</scp> ickering emulsion templates. Journal of Applied Polymer Science, 2018, 135, 46386.	2.6	16
150	Magnetic fluids' stability improved by oleic acid bilayer-coated structure via one-pot synthesis. Chemical Papers, 2016, 70, .	2.2	14
151	Adsorption of water vapor onto and its electrothermal desorption from activated carbons with different electric conductivities. Separation and Purification Technology, 2012, 85, 77-82.	7.9	13
152	Ultrahigh nitrogen-doped carbon/superfine-Sn particles for lithium ion battery anode. Journal of Materials Science: Materials in Electronics, 2020, 31, 22224-22238.	2.2	11
153	Full spectrum ultra-wideband absorber with stacked round hole disks. Optik, 2022, 249, 168297.	2.9	11
154	Hydrodeoxygenation of non-edible bio-lipids to renewable hydrocarbons over mesoporous SiO2-TiO2 supported NiMo bimetallic catalyst. Applied Catalysis A: General, 2022, 633, 118475.	4.3	11
155	Physically Close yet Chemically Separate Reduction and Oxidation Sites in Double-Walled Nanotubes for Photocatalytic Hydrogen Generation. Journal of Physical Chemistry Letters, 2019, 10, 3739-3743.	4.6	9
156	Route to Mesoporous TiO2/Graphitic Carbon Microspheres for Photocatalytic Reduction of CO2 under Simulated Solar Irradiation. ECS Solid State Letters, 2013, 2, M49-M52.	1.4	8
157	Sandwich-like mesoporous graphene@magnetite@carbon nanosheets for high-rate lithium ion batteries. Solid State Sciences, 2016, 57, 16-23.	3.2	6
158	Boosting bio-lipids deoxygenation via tunable metal-support interaction in nickel/ceria-based catalysts. Fuel, 2022, 322, 124027.	6.4	6
159	Hydrogenated Oxide as Novel Quasi-metallic Cocatalyst for Efficient Visible-Light Driven Photocatalytic Water Splitting. Journal of Physical Chemistry C, 2021, 125, 12672-12681.	3.1	5
160	Hierarchical porous photocatalysts. Interface Science and Technology, 2020, , 63-102.	3.3	4
161	Water Splitting By Photocatalytic Reduction. Green Chemistry and Sustainable Technology, 2016, , 175-210.	0.7	2
162	TiO2 supported on SiO2 photocatalysts prepared using ultrasonic-assisted sol-gel method. Materials Science-Poland, 2011, 29, 189-194.	1.0	0